

Article

Accelerating Biomanufacturing by Modeling of Continuous Bioprocessing—Piloting Case Study of Monoclonal Antibody Manufacturing

Martin Kornecki, Axel Schmidt , Lara Lohmann, Maximilian Huter, Fabian Mestmäcker, Leon Klepzig, Mourad Mouellef, Steffen Zobel-Roos and Jochen Strube *

Institute for Separation and Process Technology, Clausthal University of Technology, Leibnizstr. 15, 38678 Clausthal-Zellerfeld, Germany

* Correspondence: strube@itv.tu-clausthal.de

Received: 24 May 2019; Accepted: 25 July 2019; Published: 1 August 2019



Abstract: An experimental feasibility study on continuous bioprocessing in pilot-scale of 1 L/day cell supernatant, that is, about 150 g/year product (monoclonal antibody) based on CHO (Chinese hamster ovary) cells for model validation is performed for about six weeks including preparation, start-up, batch, and continuous steady-state operation for at least two weeks stable operation as well as final analysis of purity and yield. A mean product concentration of around 0.4 g/L at cell densities of 25×10^6 cells/mL was achieved. After perfusion cultivation with alternating tangential flow filtration (ATF), an aqueous two-phase extraction (ATPE) followed by ultra-/diafiltration (UF/DF) towards a final integrated counter-current chromatography (iCCC) purification with an ion exchange (IEX) and a hydrophobic interaction (HIC) column prior to lyophilization were successfully operated. In accordance to prior studies, continuous operation is stable and feasible. Efforts of broadly-qualified operation personal as well as the need for an appropriate measurement and process control strategy is shown evidently.

Keywords: continuous bioprocessing (CBP); model validation; antibodies; quality-by-design (QbD); process analytical technology (PAT)

1. Introduction

The production of biopharmaceutical proteins is heavily based on batch processes, although continuous bioprocessing has been shown to exhibit significant benefits, such as improvements in agility, flexibility, quality, cost, and society [1]. The biopharmaceutical market share is dominated by oncology (104 bn. US\$), besides antirheumatic (56 bn. US\$) and antidiabetic drugs (46 bn. US\$). Two drugs of the five most successful oncological products are anticipated to be monoclonal antibodies (Pembrolizumab and Nivolumab) by the year 2024 [2].

1.1. Critical View on Current Practice

Current state of the art of monoclonal antibody manufacturing is based on a batch platform process [3,4]. This process is divided into upstream and downstream processing. The production of the recombinant target protein is based on cell cultivation in bioreactors during the upstream processing. The objective of the subsequent downstream processing is to isolate the target protein from side components such as host cell proteins (HCPs), host cell DNA (hDNA), media components, viruses, and endotoxins by using various unit operations such as centrifugation, filtration, and chromatography [4–9].

This platform process includes fed-batch suspension cultivation of mammalian cells up to 20,000 L bioreactor volume, centrifugation and depth filtration as cell harvest, protein A affinity chromatography as capture, cation exchange chromatography (CIEX) as intermediate purification, and hydrophobic interaction chromatography (HIC) as polishing step [10–12]. In addition, orthogonal virus inactivation steps using low pH hold and virus filtration are implemented to minimize immunogenicity [3,4]. Subsequent to the protein A affinity chromatography and low pH hold for virus inactivation, diafiltration needs to be performed to load the following CIEX [3].

To evaluate each unit operation, certain parameters need to be characterized. These include resolution, speed, capacity, and recovery [13]. The main goal of a certain unit operation during downstream processing varies depending on its separation task.

Looking at the established platform process, the chromatographic steps will reach their capacity limit due to increasing product concentrations achieved by upstream processing optimization (i.e., cell engineering, media and process parameter optimization). This limitation is widely known as downstream bottleneck [7,14–18]. With increasing product concentration, the specific costs (€/kg) of the upstream and downstream processing declines. However, with higher product concentrations the platform downstream process will reach its efficiency optimum. Increasing the product concentration even more leads to a significant shift of cost of goods (COGs) from upstream to downstream processing [4,19–21].

Continuous bioprocessing circumvents the aforementioned downstream bottleneck and batch scale-up problems by increasing the productivity and flexibility of each unit operation with a simultaneous increase in product quality resulting from continuous product processing (i.e., short hold times) [6,14,21–33]. The FDA (U.S. Food and Drug Administration), EMA (European Medicinal Agency), ICH (International Council for Harmonization of Technical Requirements for Pharmaceuticals for Human Use), and various industrial working groups have started to publish guidelines (ICH Q8 to Q11) to increase product quality during manufacturing and; therefore, promoting continuous bioprocessing [34–39]. In addition, this productivity increase reduces the overall specific COGs of about 88% (see Figure 1). An additional benefit could be gained of about another 15% decrease by implementing alternative process concepts like ATPE (aqueous two-phase extraction) combined with iCCC (integrated counter-current chromatography), which is depicted in Figure 1.

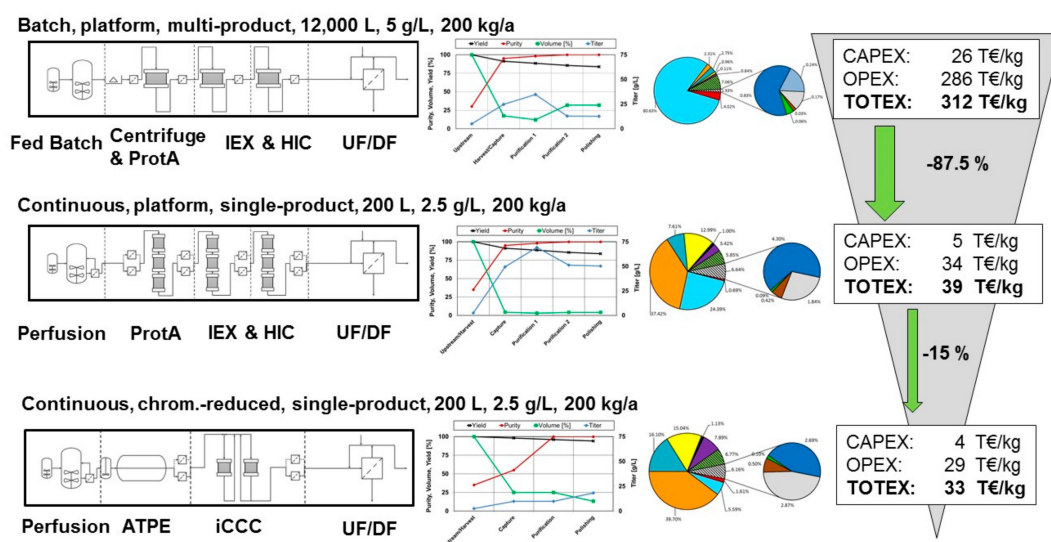


Figure 1. Schematic cost comparison between batch and continuous operational mode for the manufacturing of monoclonal antibodies [6]. ProtA (protein a chromatography), IEX (ion exchange chromatography), HIC (hydrophobic interaction chromatography), UF (ultrafiltration), DF (diafiltration), ATPE (aqueous two-phase extraction), iCCC (integrated counter-current chromatography), CAPEX (capital expenditures), OPEX (operating expenditures), TOTEX (total expenditures).

To implement continuous bioprocessing in an industrial environment, there is not only a need for guidelines but also for case studies, which show the feasibility and highlights challenges, which needs to be addressed (e.g., sterility, operational costs and process development) [40].

This article; therefore, addresses and highlights the challenges of operational costs and process development for the continuous bioprocessing of a monoclonal antibody by alternative unit operations, which has not been published before.

1.2. Process Development of an Alternative Continuous AAC Process

The tendency to substitute chromatography as purification step is called ABC (anything but chromatography). As current state, the substitution of all chromatographic steps seems to be difficult due to their robust and efficient operation. Therefore, AAC (anything and chromatography) is the most logical procedure for the implementation of alternative unit operations to substitute certain chromatographic steps [15]. For this, the implementation of ATPE for capture and protein A affinity chromatography alternative, as well as the iCCC for a combination of the CIEX and HIC in a continuous operating mode, is investigated in this case study. Seen in isolation, the feasibility and implementation of ATPE was already shown in pilot-scale manufacturing of a 200 L cultivation [41]. Since the iCCC is based on standard chromatographic devices, scale-up procedures are well documented [42,43]. The operational feasibility and processing benefits of iCCC are documented in the literature as well [44].

In terms of process development, a favorable process design space can be established by introducing risk assessments for each unit operation, supported by process modeling and design of experiments (DoE) [1,38,45–48]. The development of control strategies for an advanced process control based on the process analytical technology (PAT) initiative is essential for a robust automatization of each unit operation and; therefore, favorable for a global process optimum. The additional data from implementing PAT techniques enable the possibility for further optimization of the process and the generation of advanced control strategies. For this purpose, the data of each unit operation must be accessible. Therefore, standardized communication methods such as OPC UA are needed, simplifying the implementation/integration of new methods. This allows not only the evaluation of a single unit operation but also of the whole process [24,49–51].

During cell cultivation, important attributes for PAT approaches include process parameters (e.g., gas flow, pH, pO₂) and variables (e.g., substrate/metabolite/product concentration, biomass/viability). The overall objective is to control critical process parameters (CPP) that influence the cellular growth rate μ , production rates of the product, host cell proteins, and metabolites, as well as product quality (e.g., post-translational modifications, structure, and efficacy). Therefore, the real-time monitoring of bioreactors is essential for an efficient, well controlled, robust bioprocess [1,52].

During aqueous two-phase extraction, important attributes for PAT approaches include process parameter such as conductivity, pH, and turbidity of the light and heavy phase. Each parameter has to be kept within certain critical ranges to assure constant product quality. The pressure drop alongside the static mixer line must also be monitored to ensure that blockage or insufficient mixing can immediately identified [1].

For batch ultrafiltration and diafiltration, the main PAT targets are obviously pressures (feed, permeate and retentate) in order to know the transmembrane pressure and measurement of the steams entering and leaving the membrane cassette to monitor separation performance. But to extend the information on other process variables, especially in case of diafiltration, implementation of conductivity, density and inline concentration sensors like ATR-FTIR (attenuated total reflection Fourier transform infrared spectroscopy) would allow a much more controlled process, which could be ended based on solution properties (salt concentration, density, product concentration) and not just assumptions based on preliminary tests.

Due to the fact that precipitation processes and its kinetics are not well understood yet, PAT becomes even more vital for this unit operation. Kornecki et al. [52] used a turbidity probe for cell density, which seems to be a promising approach for online determination of precipitation progress

also simultaneous. Throughout further studies, ATR-FTIR, Raman, NIR (near-infrared spectroscopy), and MIR (mid-infrared spectroscopy) are also promising for such data-rich processes and will be tested for precipitation.

For the chromatographic separation, the inline concentration measurement (ICM) is an important PAT approach [53]. With this technique, the measured UV (ultraviolet) signals result in real protein concentrations. Due to this, the cut points for the separation can be adapted for each cycle in real-time. This results in better purities due to small changes of the retention time. With the time-based cut points these changes normally result in lower purities. In addition, for iCCC runs, it is possible to obtain conductivity data and determine the mean salt concentration in the fraction. With this information, it is possible to dilute the pooled fraction to the correct conductivity.

During lyophilization, two different pressure sensors measure the chamber pressure. The different kinds, namely the capacitive method and the Pirani sensor, enable comparative pressure measurement. The Pirani sensor depends on the composition of the atmosphere. If no more ice sublimates and both pressure sensors show the same value, the drying step is concluded. This, in combination with pressure rising tests, allow to determine the endpoint of both drying steps and present an important PAT approach. These results can be compared to clocked scaling of a single vial as well as wireless measurement of the product temperature. These data can be used as stepping criteria between sections and result in more robust, shorter processes.

In terms of economics (i.e., operational costs for academia), such piloting studies with at least two PhD students per shift at four- to five-shift continuous operation is challenging, but not in an industrial environment, since the development of continuous manufacturing can be implemented swiftly into the already established research and development workflow (i.e., infrastructure, personnel, investment). The presented study was operated once for at least two weeks stable operation, which corresponds to 14 batches at 1 L batch volume. Stable steady-state operation is shown for 100 h, which equals four reproducible batches.

The set-up of the investigated process is shown in Figure 2. The flowsheet in Figure 3 depicts all relevant operation parameters and equipment specifications of the operated process. A summary is presented in Table 1.



Figure 2. Laboratory set-up of the continuous production of a monoclonal antibody. ATPE (aqueous two-phase extraction), SPTFF (single-pass tangential flow filtration), IPC (interprocess communication), iCCC (integrated counter-current chromatography), DF (diafiltration), Lyophil (lyophilization).

Table 1. Operation parameters and equipment specifications of the operated process. ATPE (aqueous two-phase extraction).

Cultivation	ATPE	Diafiltration	Chromatography	Lyophilization
Dimensions				
2 L working volume 1.85 h/d 54 mm stirrer	175 mL hold-up DN35	30 kDa 200 cm ² Hydrosart®	10 cm height 1.6 cm diameter Toyopearl SP-650 (s) TSKgel® phenyl-5PW	2025 cm ² shelf area 6R vials (1 mL)
Process Parameters				
36.8 °C 433 rpm pH 7.1 5% CO ₂ 60% pO ₂ 200 cm ³ /min air 4800 FAU	0.7 g/min feed 0.2 g/min PEG 400 1.2 g/min PO ₄ buffer	2 bar feed 1 bar retentate 1.5 bar TMP	1 mL/min loading 2 mL/min wash, elution, regeneration 3 CV gradient elution	Heating/cooling rate 1 K/min Shelf temperature 25 °C (prim. dry.) 35 °C (sec. dry.) 0.076 mbar chamber pressure

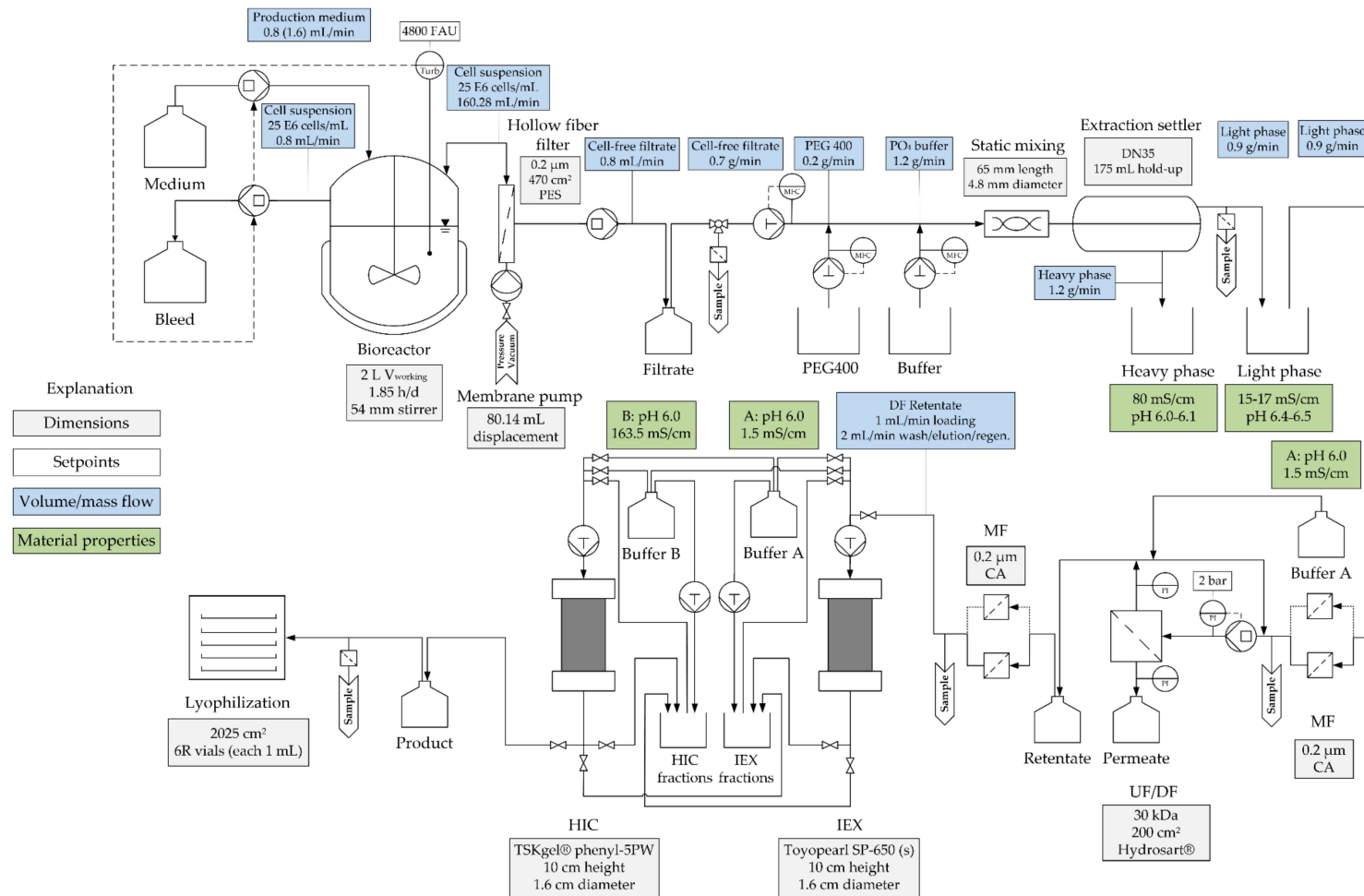


Figure 3. Process flowsheet of the continuous production of a monoclonal antibody. PES (polyethersulfone), PEG (polyethylene glycol), DN (diameter nominal), DF (diafiltration), MF (microfiltration), CA (cellulose acetate), UF (ultrafiltration), IEX (ion exchange chromatography), HIC (hydrophobic interaction chromatography), Turb (turbidity), MFC (mass flow controller), PI (pressure indicator).

2. Materials and Methods

All unit operations were tested a priori separated from the other process steps. Afterwards, 1–2 weeks of pre-cultures and start-up was needed. After 5 days batch startup, the shift towards a stable perfusion operation point was achieved and sustained for over about 1 additional week. In total, 2 weeks of continuous operation was performed. Analysis was made in parallel, nevertheless an additional 3 weeks for analytics of all data sets were needed, which can be reduced by an implementation of suitable process analytical technology (PAT) approaches [52,54].

2.1. Cell Culture

Chinese hamster ovary cells (CHO DG44) were used to produce a monoclonal antibody. The culture conditions were 36.8 °C, pH 7.1, 60% pO₂, and 433 rpm (3-blade segment stirrer impeller with a diameter of 54 mm and blades at an angle of 30°, bbi-biotech GmbH, Berlin, Germany).

The cultivations were carried out in 1 L serum-free, commercial medium (CellcaCHO Expression Platform, Sartorius Stedim Biotech GmbH, Göttingen, Germany) in 2 L glass bioreactors (Biostat® B, Sartorius Stedim Biotech GmbH, Göttingen, Germany), controlled via a digital control unit (DCU, Biostat® B, Sartorius Stedim Biotech GmbH, Göttingen, Germany). Pre-cultures were grown in shaking flasks in serum-free medium.

Regarding continuous cultivations, an alternating tangential flow filtration (ATF) perfusion system was used for cell retention. Perfusion was initiated as soon as the viable cell concentration reached 2×10^6 cells/mL. A volume exchange of $1 V_{\text{Reactor}}/d$ was maintained throughout continuous cultivation. The viable cell concentration was kept constant at certain cell concentrations by using an in-situ turbidity probe (transmission, 880 nm, HiTec Zang GmbH, Herzogenrath, Germany). Cell concentration was repeatedly quantified using a hemocytometer (Neubauer improved, BRAND GmbH + CO KG, Wertheim, Germany) and trypan blue solution (0.4%, Sigma-Aldrich, St. Louis, MO, USA) as dye for the detection of dead cells.

2.2. Extraction

The phase-forming components polyethylene glycol 400 (Merck KGaA, Darmstadt, Germany), phosphate buffer, and CCF (cell culture fluid) were combined in two T-pieces by three piston pumps (LaPrep P130, VWR, Darmstadt, Germany) according to mass-flow measurements (Mini Cori-Flow, Bronkhorst Deutschland Nord GmbH, Kamen, Germany), and mixed by static helix mixers (ESSKA.de GmbH, Hamburg, Germany). The mass-flow for each component was recorded during the process by a Labbox (Labbox 3 M, HiTec Zang GmbH, Herzogenrath, Germany). At the outlet of the separator, the phases were collected separately from each other. The settler has a nominal diameter of 35 mm and a length of 175 mm, resulting in approximately 175 mL of hold-up volume including the dead volume of necessary tubing. During the experiment, samples were taken in order to detect changes in product yield or purity over time. pH (InoLab pH 720, WTW, Weilheim, Germany), and conductivity (InoLab pH 720, WTW, Weilheim, Germany) were measured for each sample.

2.3. Diafiltration

To change the surrounding medium between the ATPE and the chromatographic separation, a diafiltration in batch mode was used. For this, the light phase of the ATPE stream was collected every 4 h and filtered with a 0.2 µm sterile filter using a CVC 3000 vacuum pump (Vacuubrand, Wertheim am Main, Germany). After sterilizing, the light phase was diluted with the target buffer (20 mM sodium dihydrogen phosphate/disodium phosphate buffer, pH 6.0) to lower the viscosity and increase initial filtration performance. Subsequently the volume was exchanged at least 5 times with the same buffer using a Sartorius SARTOFLOW® Slice 200 Benchtop system (Sartorius, Göttingen, Germany). For fixing of the 30 kDa Sartocon Slice 200 Hydrosart® membrane cassette, two stainless steel plates in the Sartocon® Slice 200 Holder (Sartorius, Göttingen, Germany) were used with a torque of 20 nm

to ensure uniform holder compression. Every buffer exchange was performed at constant feed and transmembrane pressure (TMP). The feed pressure was kept at 2 bar and the TMP at 1.5 bar. Finally, a concentration step reduced the protein solution to its initial volume at the same process pressure levels. Samples were taken from both the sterile filtered starting solution and the concentrated product solution to evaluate the experiments. In addition, the flux was recorded online by measuring the mass development of the permeate with a scale. After each diafiltration step the cassettes were cleaned with 1 M NaOH for 1 h and equilibrated with target buffer before it was used again.

2.4. Precipitation

Precipitation was accomplished from light phase (LP) after ATPE and from CCF directly after cultivation using a PEG 4000 stock solution (40 wt%, Sigma Aldrich). For dissolution, a 20 mM sodium dihydrogen phosphate/disodium phosphate buffer at pH 6.0 was utilized, which was the needed buffer in the following purification step (IEX).

At first, preliminary experiments were carried out to determine precipitation duration, amount of PEG needed in percentage of weight to result in complete precipitation of target protein, and to measure the required time for dissolution. A turbidity sensor was used for online detection of precipitation progress. After 120 min, the signal was at a constant level, which led to the assumption that precipitation was completed. The experimental set-up for the precipitation unit is shown in Figure 4.

Firstly, base material was introduced into the crystallizer and stirred at 300 rpm. In prevention of foaming due to PEG 400 fraction in LP, too rapid stirring had to be avoided. Afterwards, PEG 4000 stock solution (40 wt%) was added until the mixture was adjusted to a final PEG content of 12 wt% respectively to protein. This led to an immediate precipitation and increase of turbidity. After 120 min precipitation was completed, succeeding precipitate and supernatant were separated by a hollow fiber module with a pore size of 0.2 μm (470 cm^2). Permeate was proceeded further into a waste tank. This step was declared as loading state of the hollow fibers. After loading, the precipitate was purified with an additional washing step utilizing 16 wt% PEG 4000 solution. Subsequently, dissolution was carried on by recycling IEX buffer for 10 cycles, with equal buffer volume as applied feed volume. Afterwards, the loaded IEX buffer was filtered through the same hollow fiber module into a product tank. During continuous study, precipitation was conducted once a day.

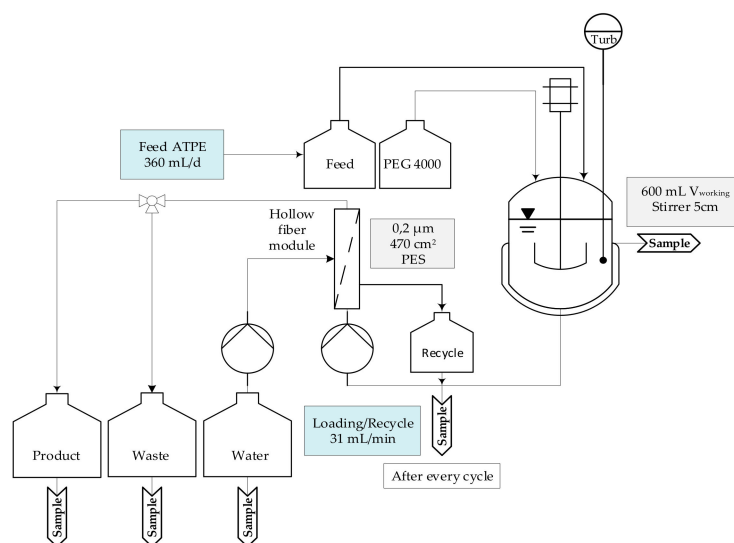


Figure 4. Experimental set-up of precipitation unit using a hollow fiber module to capture mAb (monoclonal antibody) precipitate and subsequently using IEX (ion exchange chromatography) buffer for dissolution and preparation to the next downstream purification step. PES (polyethersulfone), ATPE (aqueous two-phase extraction), PEG (polyethylene glycol), Turb (turbidity).

2.5. Chromatographic Separation

For the preliminary studies, a 1.5 CV (column volumes) wash step followed by 5 CV gradient was used. For the regeneration and the equilibration, 3 CV were used with an injection volume of 4 mL.

For the ion-exchange chromatography, a 0.9 CV gradient separation from 0% B up to 15% was utilized followed by 1.5 CV regeneration at 50% B and 3 CV equilibration. For hydrophobic interaction chromatography, a 2.2 CV gradient from 50% to 15% B was used followed by 3 CV regeneration and 3 CV equilibration at 50% B. For the recycle of the HIC-fraction, the same amount of fraction volume was added with buffer B. For the ion-exchange fraction, twice the fraction-volume buffer A was added.

2.6. Lyophilization

The preliminary tests were carried out with an IgG standard solution with concentrations of 0.5, 1, and 1.5 g/L. The solutions were supplemented with 25 g/L of sucrose. For the process, 6R DIN/ISO vials were used and were filled with 1 mL solution each.

As freeze-drying unit an Epsilon 2–6D LSCplus with LPC control software of the company (Martin Christ Gefriertrocknungsanlagen GmbH, Osterode, Germany) were used. The unit is equipped with diverse process analytical tools:

- A scale (“LyoBalance” measuring the weight loss of a single vial)
- Up to eight wireless temperature sensors (“Wireless Temperature Measurement”, WTM)
- A resistance sensor (“LyoRx” to determine the freezing point)
- Two different pressure sensors (capacity and Pirani, enabling comparative pressure measurement)

The freeze-drying process was adapted from literature and is shown in Table 2 [55].

Table 2. Freeze-drying process. Prim. (primary), Sec. (secondary), p_{chamber} (chamber pressure), T_{shelf} (shelf temperature).

Phase Section	Freezing			Annealing				Prim. Drying			Sec. Drying	
	1	2	3	4	5	6	7	8	9	10	11	12
Time (hh:mm)	00:00	01:10	02:00	00:25	01:00	00:25	02:00	00:10	00:20	50:00	01:00	15:00
T_{shelf} (°C)	25	−45	−45	−20	−20	−45	−45	−45	−25	−25	35	35
p_{chamber} (mbar)	–	–	–	–	–	–	–	0.076	0.076	0.076	0.076	0.076

The secondary drying temperature was lowered by 5 K to avoid product harming. The section time was concurrently increased by 5 h. Additionally, the weight of sample vials, product temperature, and chamber pressure were monitored. For the preliminary studies, an IgG standard solution (gammanorm[®], octapharma GmbH, Langenfeld, Germany) was used. The contained solution consists of at least 95% IgG. The other constituents present the stabilizing substances, namely glycine, sodium chloride, sodium acetate, polysorbate 80, as well as water for injection.

2.7. Buffers and Columns

Thousand grams of phosphate buffer was used as phase forming component (ATPE) contains 262.09 g disodium phosphate dihydrate (p.A., Merck, Darmstadt, Germany), 198.39 g potassium dihydrogen phosphate (p.A., Merck, Darmstadt, Germany), and 539.52 g deionized water.

The chromatographic experiments were carried out in 20 mM sodium dihydrogen phosphate/disodium phosphate buffer at pH 6.0. This buffer was used as buffer A for equilibration of the ion-exchange chromatography and for elution of the hydrophobic interaction chromatography. For elution on ion-exchange and equilibration on hydrophobic interaction, 2 M ammonium sulfate was added as buffer B.

The iCCC experiments were carried out using a self-packed Superformance[®] 300-16 column (Götec-Labortechnik GmbH, Bickenbach, Germany). For ion-exchange the column was packed with

Toyopearl SP-650 (s) (Tosoh Bioscience GmbH, Griesheim, Germany). For hydrophobic interaction chromatography TSKgel® phenyl-5PW was used as adsorbent. Both columns were packed to a bed height of 10 cm. The volumetric flow rate was 2 mL/min and for the feed loading the flow rate was reduced to 1 mL/min.

For analytical size-exclusion chromatography (SEC), a buffer containing 100 mM sodium sulfate and 100 mM phosphate buffer at pH 6.6 was utilized. All salts were obtained from Merck KGaA, Darmstadt, Germany. Analytical SEC columns Yarra® SEC-3000 (3 µm, 300 × 4.6 mm) were obtained from Phenomenex Inc., Torrance, CA, USA. Protein A chromatography was performed with PA ID Poros® Protein A Sensor Cartridges (Applied Biosystems, Waltham, MA, USA).

The sucrose used in lyophilization was obtained by CarlRoth and had a purity of 99.5%.

2.8. Devices and Instruments

The experimental setup consisted of two standard VWR-Hitachi LaChrom Elite® HPLC systems (VWR®, Darmstadt, Germany). One system was equipped with a quaternary gradient pump L2130, Autosampler L-2200 and diode detector L-2455. The other system contained also a quaternary gradient pump L2130 and a UV detector L-2400. Both systems were connected and used for the integrated countercurrent chromatography.

Analytical Protein A and SEC measurements were carried out using two Agilent 1100 HPLC systems (Agilent Technologies, Waldbronn, Germany) equipped respectively with an autosampler (G1329A; G1313A), a column oven (G1316A; G1316A), diode detector (DAD, G1330B; G1315B), two binary pumps (G1312A; G1312A), and a vacuum degasser (G1312A).

3. Results and Discussion

3.1. Cell Culture

A schematic overview of the perfusion cultivation can be seen in Figure 5. At high viabilities (>95%), turbidity can be used for the online monitoring of viable cell concentration. Therefore, an online control was implemented by a turbidity threshold. One operating point (4800 FAU) was chosen for the control of viable cell concentration, which represents a viable cell concentration of 25×10^6 cells/mL. As soon as turbidity surpassed respective threshold, a bleed pump was automatically triggered. The sum of permeate and bleed volume flow resulted in a higher feed volume flow to maintain the culture volume. An ATF ratio (ratio between permeate volume flow and ATF flow rate) of 200.35 was reached at an ATF flow rate of 160.28 mL/min by a pump displacement of 80.14 mL at one pump cycle per minute (one cycle is defined as vacuum exhaust and pressurized displacement of the entire pump volume). The viable cell concentration (1×10^5 cells/mL) and turbidity (FAU) is depicted in Figure 6.

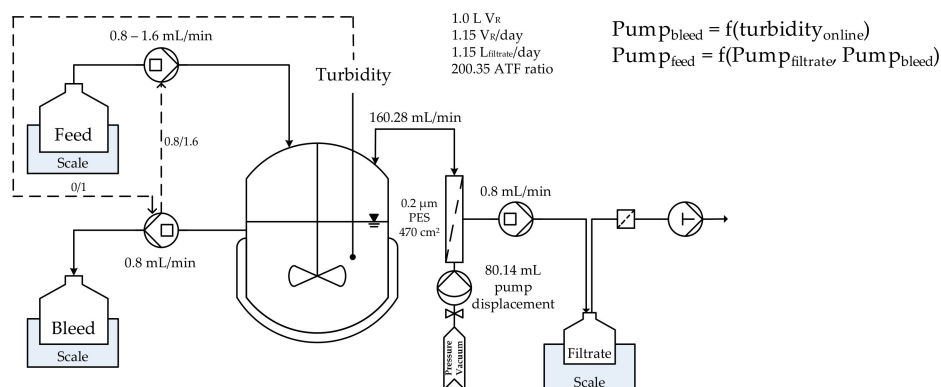


Figure 5. Schematic overview of the turbidostat perfusion cultivation including control strategy for viable cell concentration via turbidity, feed, and bleed pump.

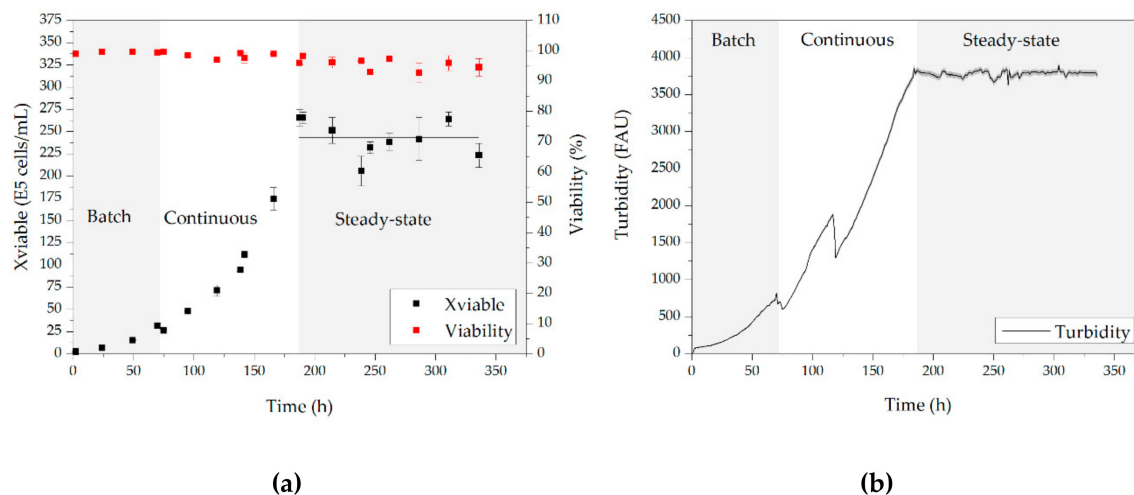


Figure 6. Viable cell concentration, cell viability (a) and turbidity (b) during continuous cultivation of CHO DG44. The horizontal line during steady-state cultivation depicts the mean viable cell concentration of $243.03 \pm 19.63 \times 10^5$ cells/mL. Measurement uncertainty of turbidity ($\pm 3\%$) is indicated as a grey enveloping curve. Error bars depict the double determination of cell concentration and viability.

The correlation between viable cell concentration (1×10^5 cells/mL) and turbidity (FAU) is depicted in Figure 7. Viable cell concentration can be expressed in the form of a simple linear regression depending on online turbidity. A coefficient of determination of 0.969 can be achieved.

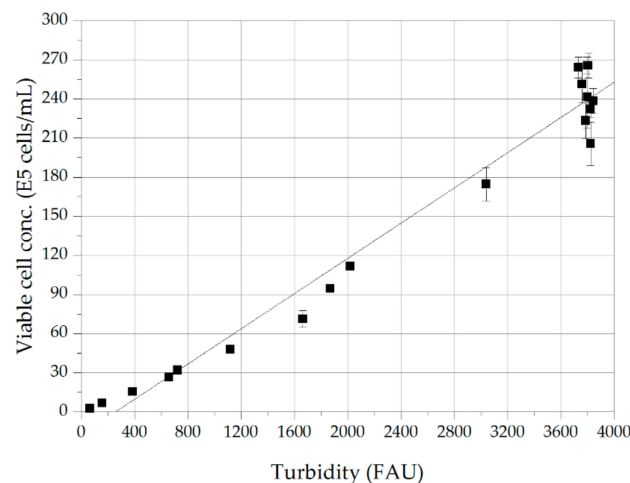


Figure 7. Linear correlation between viable cell concentration (1×10^5 cells/mL) and turbidity (FAU) with a slope of 0.068 ± 0.003 and an offset of -17.40 ± 8.01 . Error bars depict the double determination of cell concentration.

The offline determined viable cell concentration can be described by online turbidity data. The high error above 3500 FAU is due to the measurement error of the probe ($\pm 3\%$). This can be circumvented by implementing a more precise measurement probe. Nevertheless, the quasi-stationary state of this turbidostat is clearly visible and increases process understanding, control, and data quantity for an advanced mammalian cell culture.

Process-related product concentration (a) and purity (b) can be seen in Figure 8. The perfusion cultivation achieved an antibody concentration of 0.34 ± 0.05 g/L (end of batch phase), 0.70 ± 0.06 g/L (start of steady-state), and 0.50 ± 0.03 g/L (as of 240 h cultivation). The lower product concentration may be due to shorter process time in comparison to conventional perfusion cultivations (14 to 60 days). However, even at lower product concentration the volumetric productivity reaches

700.34 ± 56.85 mg/L/d (start of stationary phase) and 503.20 ± 28.45 mg/L/d (as of 240 h cultivation). This high productivity among other process characteristics (e.g., lower investment expenditures, long-term continuous cultivation) enhances the attractiveness of perfusion systems.

Figure 9 depicts offline conductivity and viability measurements (a) as well as glucose and lactate concentrations (b) during respective phase of the cultivation. As it can be seen, the conductivity is except for one outlier (120 h) in correlation with the cell viability. The outlier can be explained by evaluating the turbidity data in Figure 6. At approximately 120 h, a significant decrease in turbidity can be seen. This is based on a prior concentration (starting at approximately 100 h) of the cell concentration due to an error of the feed pump. This led to a decreased medium volume flow and subsequently to a decreased cell culture volume. Due to the cell retention system, the cell concentration increased. After 20 h the error of the feed pump was eliminated, and the culture volume was increased manually to the initial volume of 1 L. However, the conductivity measurements depict no significant increase based on decreasing viability and release of cell lysate.

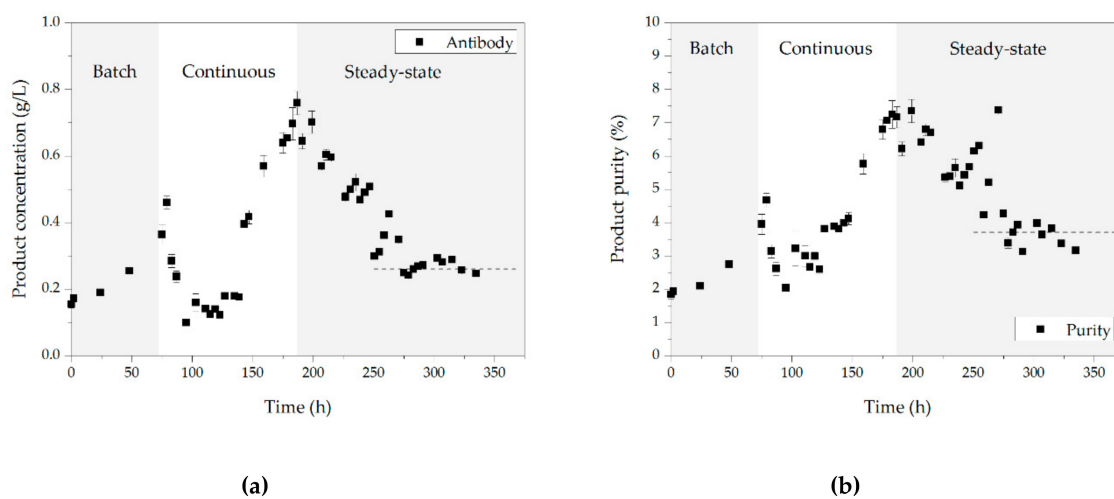


Figure 8. Product concentration (a) and purity (b) during batch, continuous, and continuous steady-state cultivation. The horizontal dashed line visualizes schematically the subsequent course of the steady-state phase after its initiation at 187 h. Error bars depict the double determination of antibody concentration and purity.

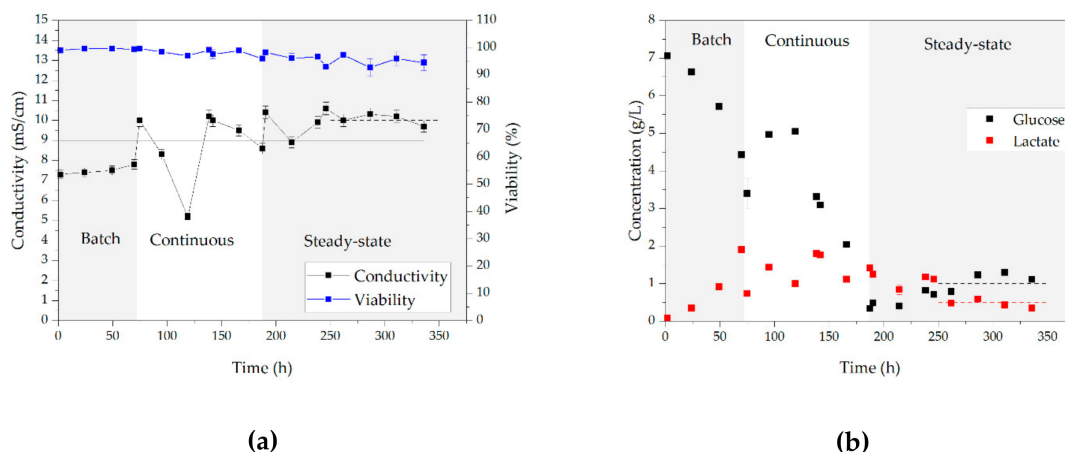


Figure 9. Conductivity, cell viability (a), and glucose and lactate concentration (b) during batch, continuous, and continuous steady-state cultivation. The horizontal solid line depicts the mean conductivity of 9.0 ± 1.4 mS/cm. The horizontal dashed line visualizes schematically the subsequent course of the steady-state phase after its initiation at 187 h. Error bars depict the double determination of conductivity, viability, glucose and lactate concentration.

The glucose and lactate concentrations in Figure 9 indicate typical progression during the batch phase. The glucose and lactate concentrations decrease and level off, respectively, as soon as the continuous operation mode was initiated. This is due to an increasing cell concentration (Figure 6) at constant perfusion rates. As soon as the glucose concentration reached below 0.5 g/L, bolus glucose concentration was fed to achieve a respective concentration of 1.0 g/L.

3.2. Aqueous Two-Phase Extraction

A schematic overview of the ATPE process set-up can be seen in Figure 10. Polymer, buffer, and CCF were pumped from their respective storage vessels into the static mixing line. After thorough mixing, the two-phase system separates into a light phase (polymer rich), which contains the product, and a heavy phase (salt rich) that contains impurities, such as DNA and lower molecular weight components (LMWC).

In Figure 11 the product concentration (a), volume flow (b) of the light phase, and conductivity and pH-value (c) is shown. The process is divided into three major stages. During batch phase of the bioreactor, no filtrate was harvested, hence ATPE was not operated. After 70 h cultivation time the perfusion begins, and the filtrate was fed into the ATPE. During this start-up period the concentration was as low as the concentration in the bioreactor, which was caused by the low cell concentration. As the concentration of cells and; therefore, product increases in the bioreactor, the same trend was observable during ATPE. As the perfusion reaches steady-state after a peak in product concentration at 192 h the concentration remained at a constant value of approximately 0.5 g/L. The conductivity and pH value are depicted in Figure 11 (right). In steady-state operation the conductivity remained at a value of 16.89 ± 0.74 mS/cm and the pH value remained constant at a value of 6.45 ± 0.04 .

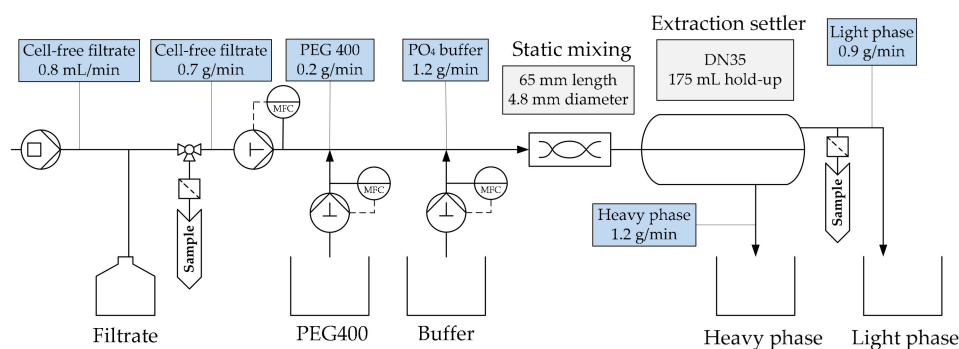


Figure 10. Schematic overview of the ATPE (aqueous two-phase extraction) process.

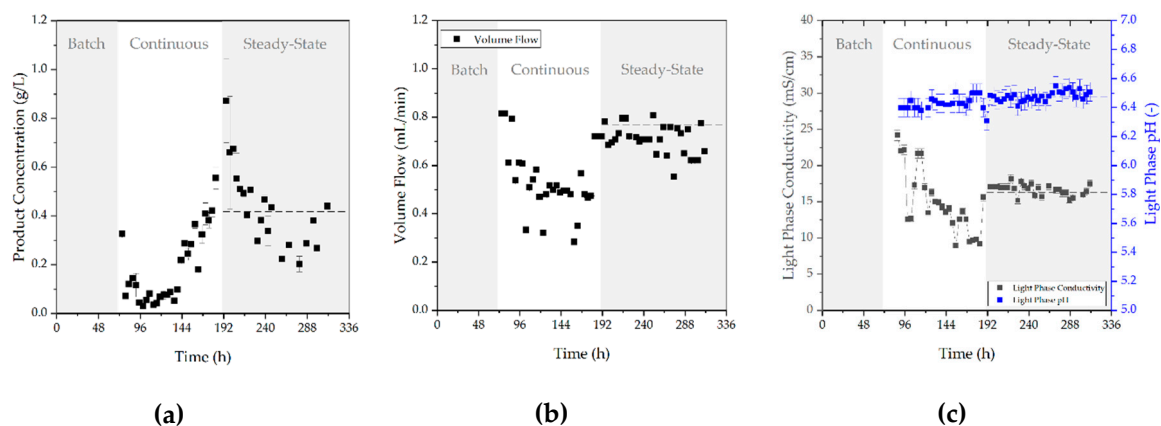


Figure 11. Product concentration (a), volume flow (b) of the light phase, and conductivity and pH-value (c) during batch, continuous, and continuous steady-state operation. The horizontal dashed line visualizes schematically the subsequent course of the steady-state phase after its initiation at 187 h. Error bars depict the double determination of each variable.

Yield (a) and purity (b) achieved in ATPE are depicted in Figure 12. The yield in the start-up phase of continuous operation (70 to 192 h process time) is low and shows larger deviations, averaging values of $32.46\% \pm 16.48\%$. This might be due to the low concentration in this process stage in the bioreactor and the factor that losses in concentration during ATPE have a stronger effect on yield, when the overall concentration is already very low. However, in steady-state operation (192 to 336 h process time), when the concentration in the bioreactor is constantly high at approximately 0.5 g/L, the yield in ATPE levels out at $87.22\% \pm 12.85\%$. Since the concentration in this phase was higher, the loss during the start-up period can be easily compensated.

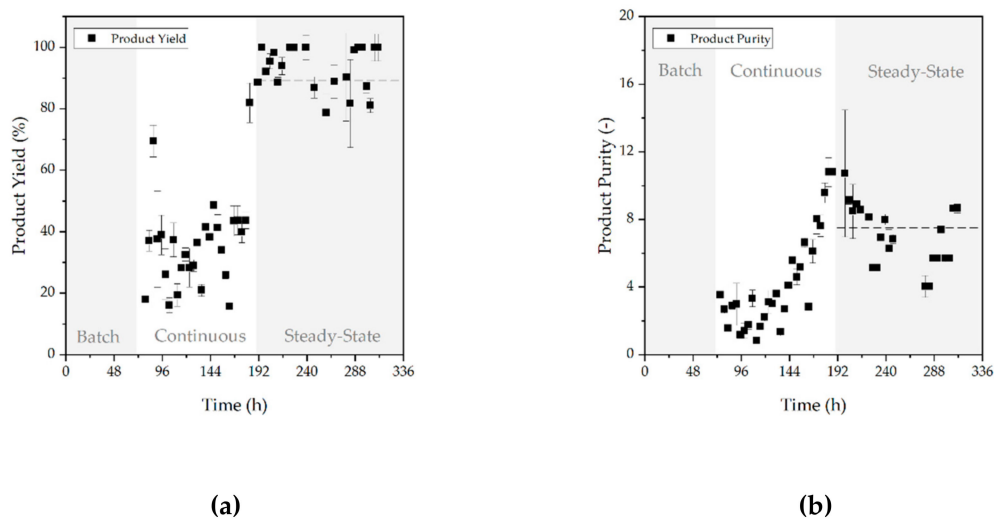


Figure 12. Yield (a) and purity (b) during batch, continuous, and continuous steady-state operation. The horizontal dashed line visualizes schematically the subsequent course of the steady-state phase after its initiation at 187 h. Error bars depict the double determination of each variable.

3.3. Diafiltration

The diafiltration step is necessary for changing the buffer of the target protein to low salt concentrations and additionally removal of PEG. A typical behavior of flux vs. time of a diafiltration step in this study is visualized in Figure 13.

Obviously, the flux increases due to removal of PEG, which increases the viscosity and lowers the filtration performance. After 10 min, the flux reaches its maximum. From this point, the filtration performance starts to decrease strongly. This is a hint for fouling due to side components blocking the pores of the membrane and possible precipitation of the target protein. The observed concentrations and purities of all diafiltration steps are depicted in Figure 14.

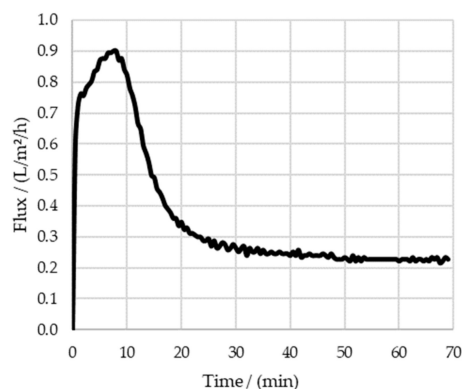


Figure 13. Exemplary flux development over time of a diafiltration step.

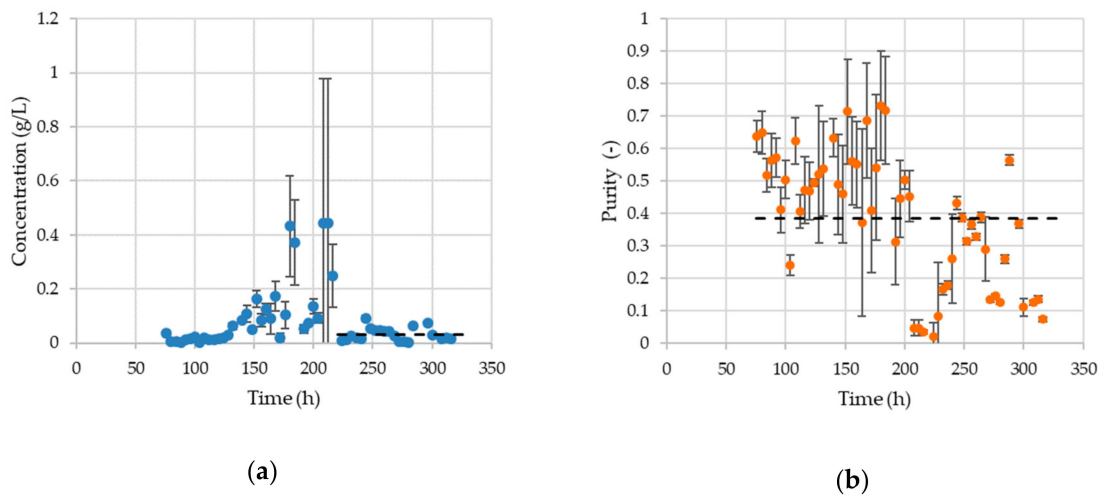


Figure 14. Development of (a) concentration and (b) purity for diafiltration steps. The dashed trendline depicts the stationary phase in terms of product concentration in (a) and the mean purity after diafiltration in (b). Error bars depict the double determination of each variable.

While the general concentration development follows the tendencies of previous process steps, the concentration in general was lower, compared to the results from ATPE. Furthermore, the yield of each diafiltration step, shows no clear course. The average value was $52\% \pm 32\%$. This great spectrum of yield was probably influenced by handling error possibilities resulting from four to five different shifts and various operators, which could be solved by appropriate training in future.

Beside the exchange of buffer, the diafiltration step also excludes side components by size. With the used membrane cassettes all molecules smaller than the cut-off of the membrane (30 kDa) pass into the permeate and are separated.

The usage of filtration methods to exchange the surrounding buffer, reaches an average purity of $45\% \pm 18\%$. It also increases the purity up to $40\% \pm 20\%$ by removing smaller molecules (e.g., DNA and proteins). Therefore, the role of the diafiltration is not only necessary to change the buffer for subsequent unit operations but also has a possibility to increase the general purity of the target molecule.

The performed diafiltration experiments show a broad distribution of resulting process variables such as yield. A continuous filtration/diafiltration method; however, would reduce the problem of handling errors. For this, single-pass tangential flow filtration systems could lead to more consistent results and developments [48].

3.4. Precipitation

In Figure 15 the achieved recovery of mAb after precipitation is shown as well as the deviation between various batches. Furthermore, a distinction between precipitation with and without a subsequent washing step after loading became obvious. It seemed that the washing step with PEG 4000 solution disturbed following dissolution and is not target-aimed in this context. Moreover, it was tested whether or not a precipitation step, as a capturing step, directly after cultivation is feasible. A complete precipitation of mAb from CCF could be accomplished because no mAb was found, neither in waste nor in supernatant, but in this instance it was not feasible to recover the mAb from precipitate. This can be seen easily in the green column in Figure 15, which displays 0% recovery of mAb. Furthermore, the concentration profile of mAb in the supernatant and its development throughout the precipitation process was analyzed with protein A chromatography. It was determined that mAb precipitation occurs very rapidly within one or two minutes. On basis of results from preliminary experiments, the precipitation time needed was set to 120 min, due to the turbidity signal. In this case, a turbidity probe is not useful to display precipitation progress, because it is not selective enough to detect the precipitation of the target protein only.

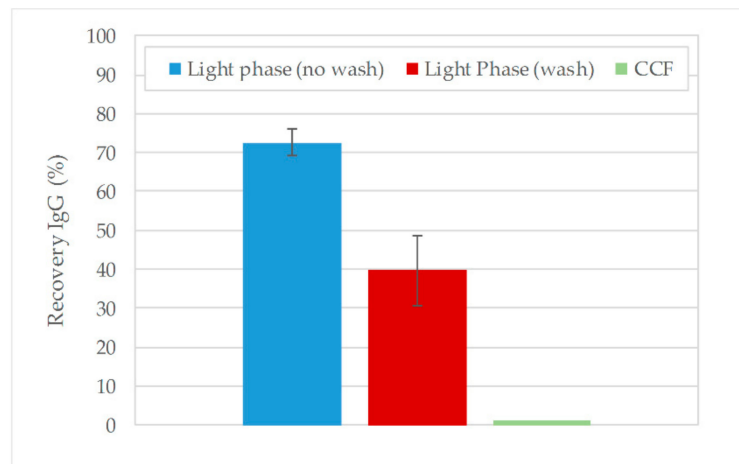


Figure 15. Recovery of mAb after dissolution with varying base materials. Dissolution without a previous washing step resulted in recovery of approximately 72.59% ($\pm 3.57\%$) mAb (blue) recovery from precipitate with subsequent washing resulted in 39.68% ($\pm 8.92\%$) recovery (red). Dissolution of precipitated CCF (cell culture fluid) was not possible (green). Error bars depict the double determination of product recovery.

To determine the host cell protein profile before and after precipitation, a SEC was used. Figure 16 shows the side component spectrum of the light phase (base material) supernatant after precipitation as well as the IEX buffer with re-dissolved mAb. The experiment displayed in Figure 16 did not include a subsequent washing step after loading. It can be seen that the recovery of mAb was achieved and a further reduction of HCPs was accomplished. Most of the HCPs remained in the supernatant and were separated from the product by filtration.

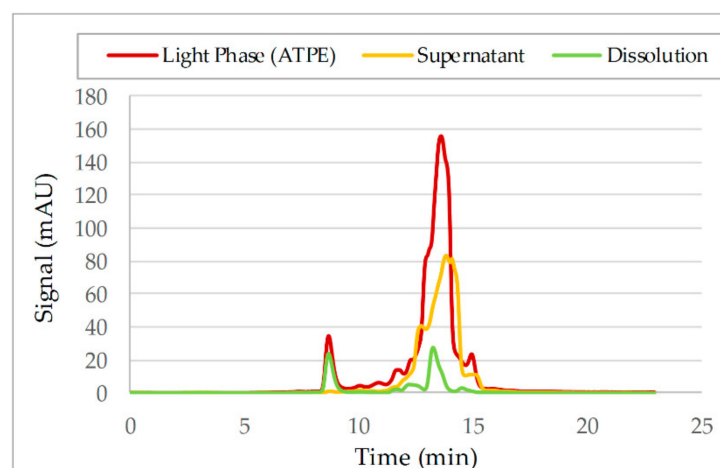


Figure 16. Recovery of mAb after precipitation. Precipitation was conducted, with LP (light phase) from ATPE (aqueous two-phase extraction) used as the base material and the absence of a washing step.

In contrast, the side component spectrum of the second precipitation attempt, including a washing step, is depicted in Figure 17. Both figures indicate that HCP spectra of supernatant in the precipitation procedure with and without washing step are highly comparable. A huge difference can be seen in the purity of product obtained from precipitation. Product purity was improved, but, simultaneously, the recovery yield of mAb was reduced ($39.68 \pm 8.92\%$). This leads to the assumption that on one hand the washing step had a positive effect on purification of mAb, because more HCPs were separated from the base material, but on the other hand it had a negative influence on dissolution.

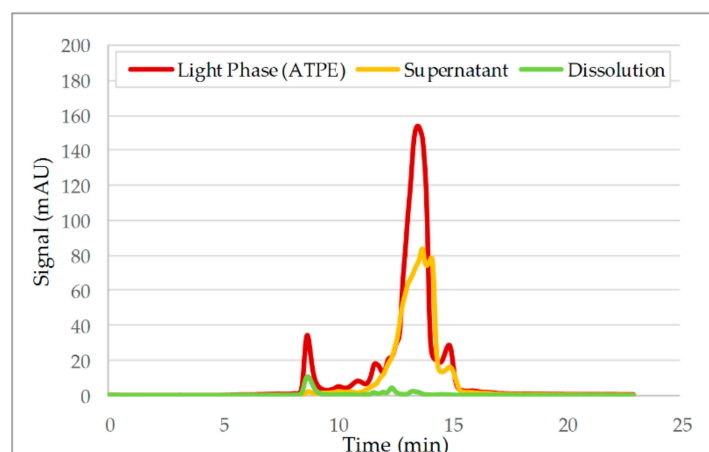


Figure 17. Recovery of mAb after precipitation. LP (light phase) from ATPE (aqueous two-phase extraction) was used as base material, including a washing step after loading the hollow fiber.

Overall, it can be said that the reduced recovery of target protein might be affiliated to the suboptimal properties of the utilized IEX buffer for dissolution. The buffer can be optimized by a pH shift to 5.5 or even 5 to enhance solubility of mAb, due to its isoelectric point (IP) around pH 8.4. Further, an increase of ionic strength up to 50 or 100 mM will lead to a salting-in effect, which might give a rise to solubility and stability of protein.

Additionally, it was tested whether complete mAb dissolution under optimal conditions given by a PBS buffer (pH 7.4) is feasible. Hence, the two different experiments described above were carried out again, but dissolution was conducted with PBS. Figure 18 shows that dissolution after precipitation with (red) and without (green) a washing step is within the deviations, which are a lot smaller compared to dissolution experiments conducted with IEX buffer. This shows in general that dissolution after precipitation is feasible and the two working procedures lead to similar results (washing: $70.22\% \pm 5.75\%$; no washing: $70.95\% \pm 13.10\%$). It is shown that dissolution kinetics with a previous washing step are slightly faster in the beginning compared to no washing. In the end both working procedures reach an analogous recovery of mAb. The missing percentages could be recovered in a second washing step with H₂O. To do so only one washing cycle was necessary. Respectively to these results, precipitation with a subsequent washing step is to be favored, due to similar yields in dissolution and higher depletion of HCPs.

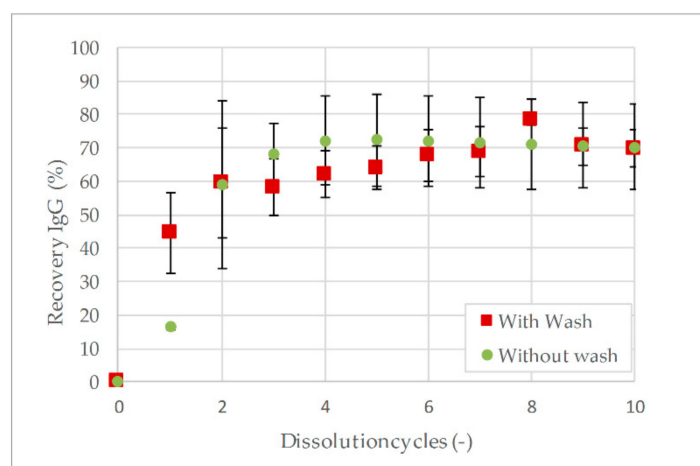


Figure 18. Feasibility study of dissolution of mAb after precipitation from LP (light phase) using PBS (phosphate-buffered saline) buffer (pH 7.4) and the experimental set-up shown above. Error bars depict the double determination of product recovery. IgG (Immunoglobulin G).

Further, it can be said that complete dissolution after precipitation is feasible, but it is highly dependent on buffer conditions.

3.5. Chromatography

At first, some preliminary tests were carried out. For this, buffers with different pH values and different gradient slopes were tested. As Figure 19 shows, buffers with pH 5.0, 6.0, and 7.0 were investigated. The buffer with pH 6.0 showed the best separation. Therefore, this pH value was chosen.

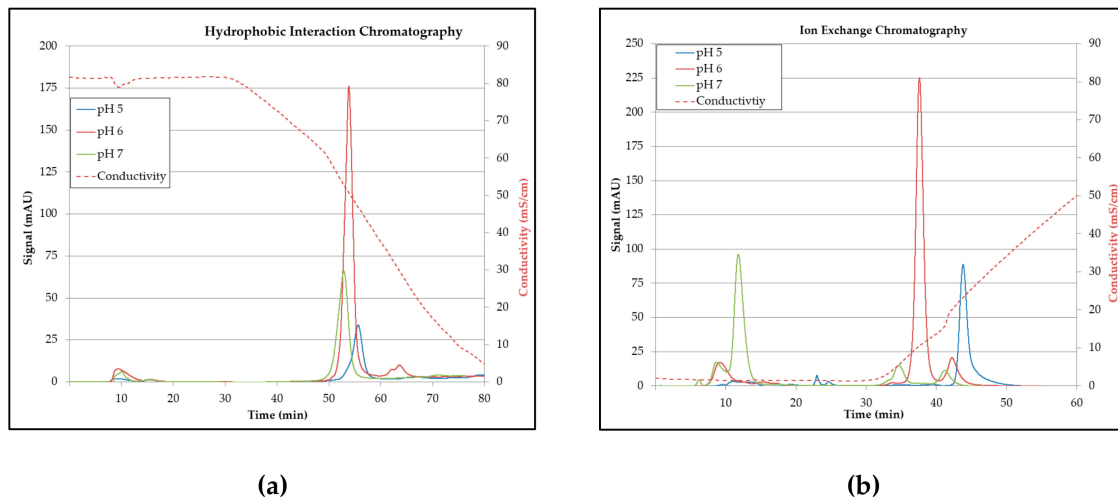


Figure 19. Influence of pH values for the hydrophobic interaction chromatography (a) and ion exchange chromatography (b).

Subsequently, various gradient slopes were tested with the designated pH value of 6.0 by varying the gradient lengths of 3, 5, and 7 CV. In Figure 20 it can be seen that even with the 3 CV gradient, a decent separation was achieved. It can also be detected that there is a potential to reduce the operating time.

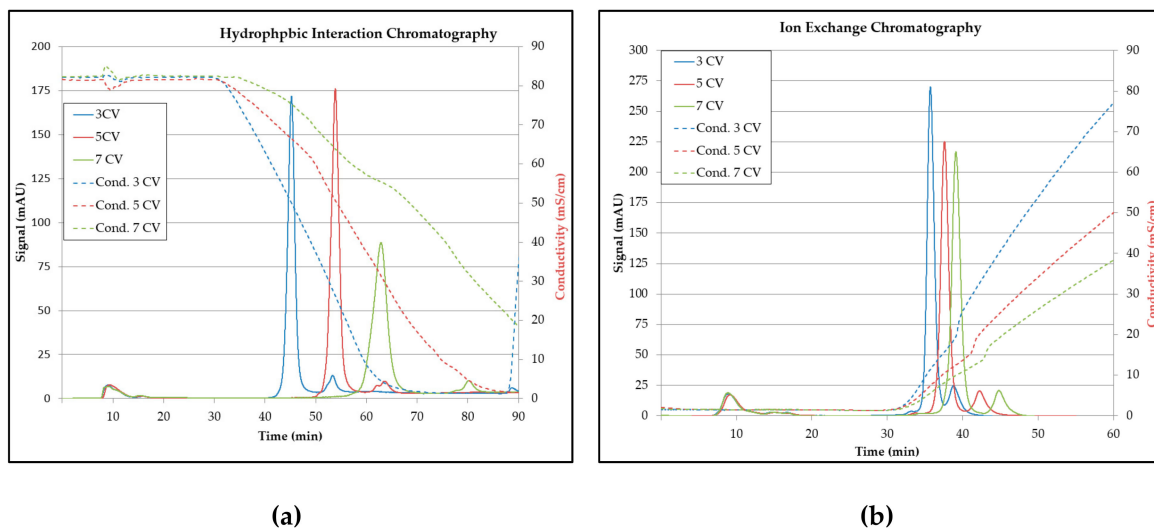


Figure 20. Influence of the gradient length for the separation: (a) For hydrophobic interaction and (b) for ion exchange. CV (column volume), Cond. (conductivity).

For the iCCC method, the wash step on both columns was eliminated. In the case of the ion-exchange, the gradient separation was carried out up to one-third of the gradient length. Thereafter,

a step-gradient to regenerative conditions were carried out. In case of the HIC method, the last one-third of the gradient were cut, so the regeneration could be started sooner. In addition, it was tested to cut the first one-third of the gradient, since the separation takes place in the middle third of gradient elution. In preliminary iCCC test runs, it was observed that a concentration occurs, which results in a widening of the product peak. Due to this effect, it is feasible to start elution sooner and, therefore, the peak was influenced by a step in the first third of the elution. Because of this, the linear elution gradient begins at 1 M ammonium sulfate (see Figure 21).

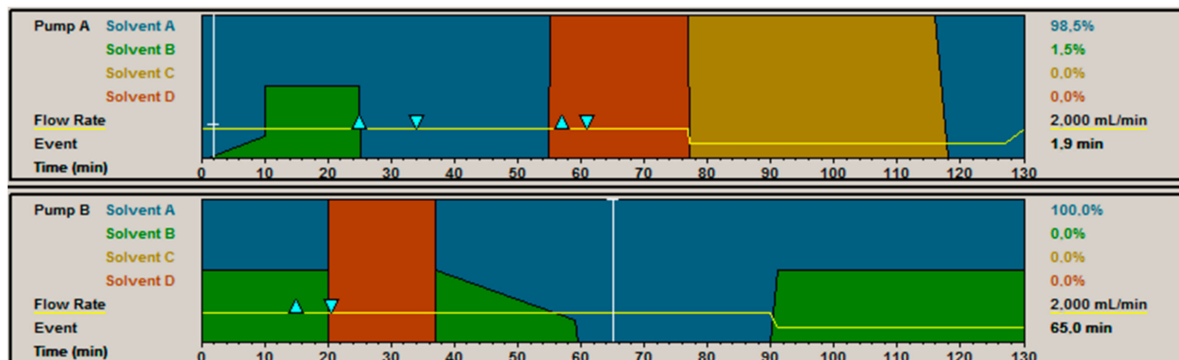


Figure 21. Method for an iCCC cycle. Solvent A is Buffer A, Solvent B is Buffer B, Solvent C is feed, and Solvent D is the recycle of the fractions. The triangle marks the addition of Buffer A into the IEX fraction and Buffer B into the HIC fraction.

In Figure 22, the concentration of the iCCC feed can be seen. For this, different DF batches (output of diafiltration) were pooled. The figure depicts three data points. The first dataset (“Start”) is the concentration directly after the addition of a new feed. The second measurement (“End”) was carried out before new feed was added. With this measurement it can be investigated if the product concentration will drop within the storage time. The third data point (“Mean”) is the mean value of both measured concentrations. With this, the mean feed concentration for the time step could be achieved and was used to calculate the yield of each cycle.

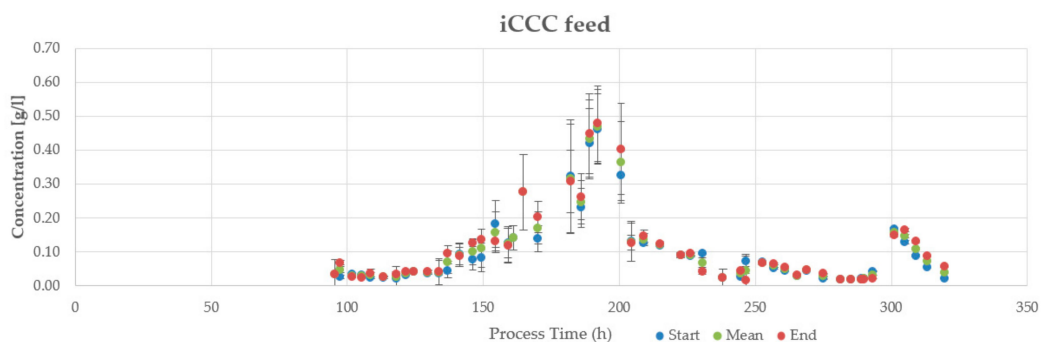


Figure 22. Feed concentration of the feed for the iCCC (integrated counter-current chromatography). Error bars depict the double determination of the product concentration.

Figure 23 shows the concentration of the product fraction of each iCCC cycle. Each fraction was analyzed by size exclusion chromatography to determine the final purity. The analysis is visualized in Figure 23. It can be seen that the purity of all cases exceeds 97%. Due to a slight shift in the retention times of the HIC, a decrease of purity can be seen. After adapting the cut points, a purity of over 99% was achieved. For all iCCC cycles, a yield of $73\% \pm 38\%$ was reached.

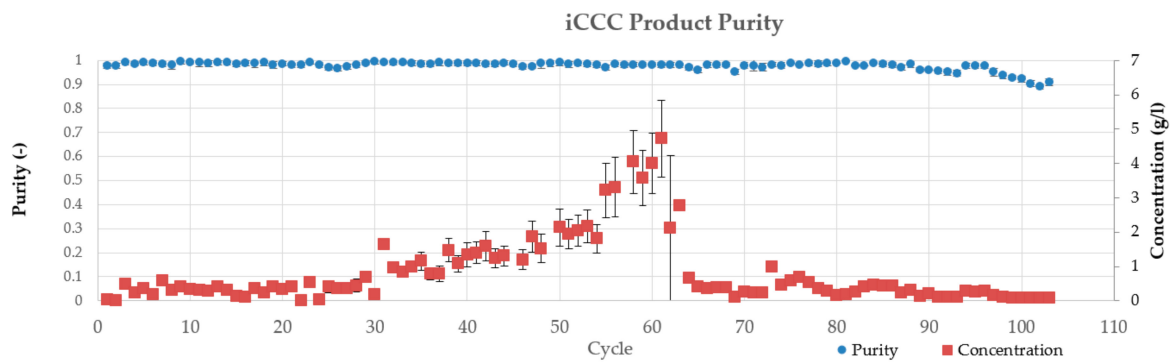


Figure 23. Product concentration and purity of the iCCC cycles. Error bars depict the double determination of the purity.

3.6. Lyophilization

The IgG standard solutions used in the preliminary tests were reconstituted and analyzed by Protein A chromatography. Results are shown in Figure 24.

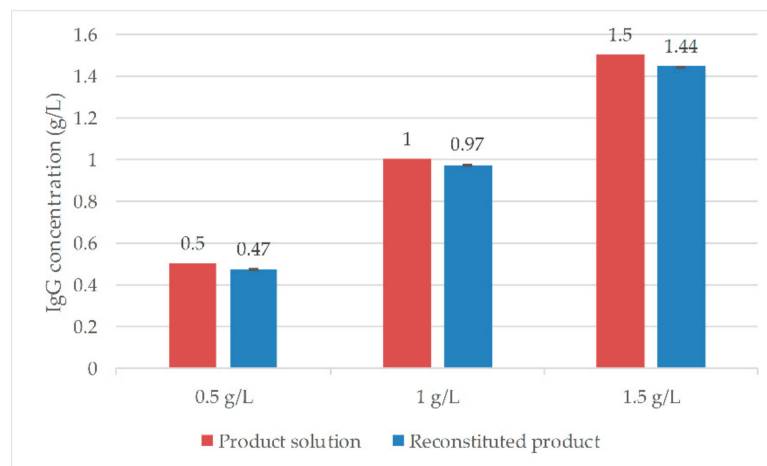


Figure 24. Preliminary study results for lyophilization. Error bars depict the double determination of the product concentration. IgG (Immunoglobulin G).

With average yields of $96\% \pm 0.4\%$, the freeze-drying cycle is considered sufficient for the drying of IgG. The only difference in the study shown here is the composition of the solution. During the tests, the IgG standard solution consisted only of the protein solution with stabilizing substances (see Section 2.6) and purified water with 25 g/L sucrose. In Figure 25, temperature and pressure profiles of the experiments are shown. The product temperature reached values higher than the shelf temperature. This can be explained by heat radiation from the surroundings. Additionally, because of that, this effect cannot be observed during secondary drying. From the convergence of the pressure measurements and the constant product temperature from 15 h, it can be concluded that drying has already been completed at this point. The dried cake showed no optical errors.

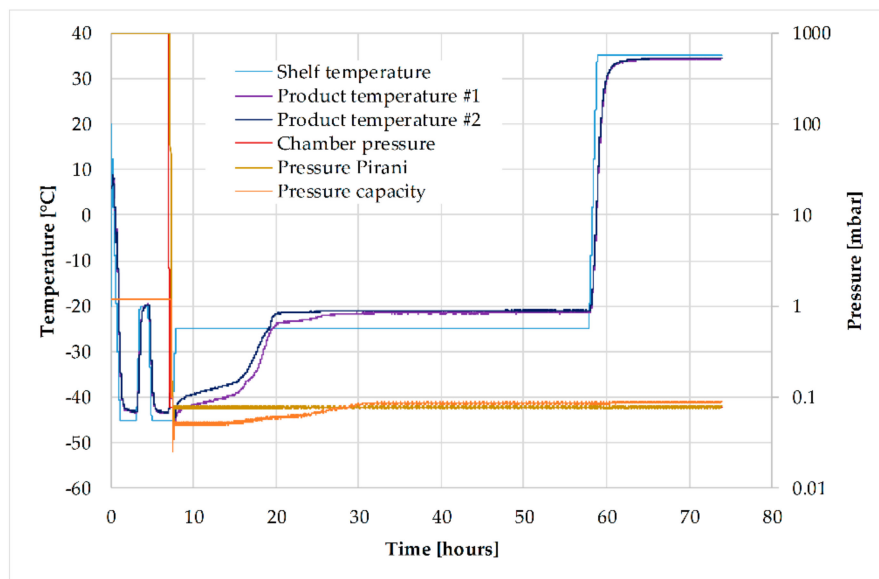


Figure 25. Temperature and pressure course during lyophilization.

3.7. Comparison between Conceptual Process Design and Experimental Data

Based on the conceptual process design (CPD) in Figure 1, a comparison of yield (%), purity (%), volume (%), and product concentration (g/L) between the experimental data of this case study and the CPD data can be seen in Figure 26. Yield, purity, volume, and product concentration of the CPD were scaled to the laboratory experiments conducted in this case study (i.e., 1 L cell culture, mean product concentration of 0.5 g/L in cultivation supernatant, 150 g_{Product}/a). Errors of $\pm 5\%$ yield, $\pm 5\%$ purity, $\pm 10\%$ product concentration, and $\pm 10\%$ volume were implemented, due to typical uncertainties in conceptual process design.

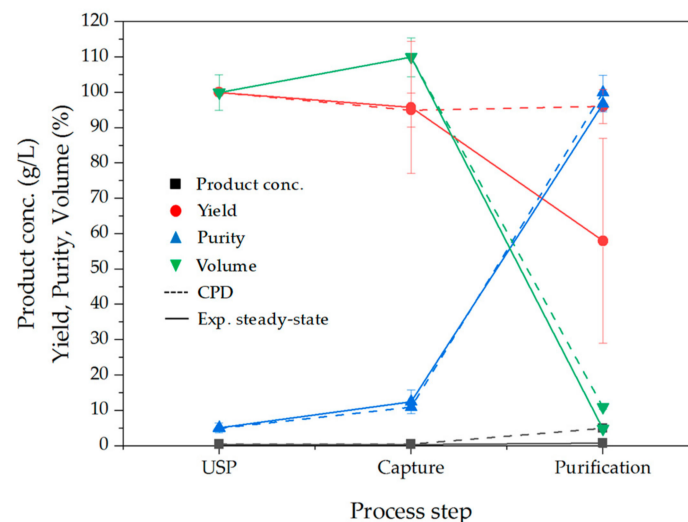


Figure 26. Comparison between conceptual process design (CPD, solid line, —) and steady-state experimental data (Exp., dashed line, - -) in terms of product concentration (black, g/L), yield (red, %), product purity (blue, %), and volume (green, %). Purity is well met, only yield and product concentration differ due to described handling and modified product concentrations during cell cultivation. Error bars depict the double determination of each variable based on experimental data and uncertainties of the CPD.

As it can be seen in Figure 26, the product concentration as well as the product purity increases with each process step (i.e., capture and purification). In addition, the volume decreases to $11.0\% \pm 0.6\%$ (CPD) and $4.8\% \pm 0.1\%$ (experimental steady-state). Product purity reaches approximately $99.9\% \pm 5.0\%$ (CPD) as well as $96.8\% \pm 2.3\%$ (experimental steady-state). The product concentration increases from 0.50 ± 0.05 to 5.00 ± 0.50 g/L (CPD) and 0.44 ± 0.15 to 0.78 ± 1.20 g/L (experimental steady-state). This discrepancy between product concentration based on the conceptual process design in Figure 1 and experimental data is mainly due to the modified product concentration during experimental cultivation (Figure 8), despite the continuous turbidostat cultivation procedure. However, even at modified product concentrations and increasing volumes during capture, the iCCC is able to significantly decrease the volume and achieve a high purity during continuous and steady-state operation [56,57].

4. Conclusions

The alternative mAb process integration concept based on ATPE and iCCC in continuous operation was successful. Additional precipitation options were discussed. Stable operation for about two weeks was achieved. Performance in yield, purity, and conformity of the mAb was reached as predicted by single unit operation studies and process modelling. Slight discrepancies were due to normal simple handling obstacles by first operation inexperience (as described in detail above).

Nevertheless, no hint could be seen that with simple fine-tuning and further personnel training experience, routine operation should be possible easily.

Further emphasis to simplify operation, improve process robustness and reduce handling efforts is; therefore, focused on PAT techniques and process control strategies by advanced process control approaches. This is a logical consequence and straight forward, as those process models are existing and have been experimentally validated [46–48,58].

Author Contributions: M.K. was responsible for cell cultivation, A.S. for ATPE, M.H. for UF/DF, L.L. for precipitation and cultivation support, F.M. and S.Z.-R. for iCCC, L.K. for lyophilization and M.M. for automation and process control. All authors operated the process and ran the analytics. J.S. was responsible for conception and supervision.

Funding: Gratefully acknowledged is the budgeting by BMWi (Bundesministerium für Wirtschaft) PTJ Jülich, Wolfgang Gahr, for enabling such studies towards industrialization.

Acknowledgments: The authors would like to especially acknowledge the help of Lukas Uhlenbrock, the troubleshooting by the laboratory team of the institute Frank Steinhäuser, workshop fine-mechanic Volker Strohmeyer, as well as measurement and control by Thomas Knebel. Automation was supervised by Christian Siemers.

Conflicts of Interest: The authors declare no conflicts of interest.

References

1. Kornecki, M.; Schmidt, A.; Strube, J. Pat as Key-Enabling Technology for Qbd in Pharmaceutical Manufacturing—A Conceptual Review on Upstream and Downstream Processing. *Chem. Today* **2018**, *36*, 44–48.
2. EvaluatePharma. *World Preview 2018 Outlook to 2024*; Evaluate Ltd.: London, UK, 2018; pp. 1–47.
3. Sommerfeld, S.; Strube, J. Challenges in biotechnology production—Generic processes and process optimization for monoclonal antibodies. *Chem. Eng. Process. Process Intensif.* **2005**, *44*, 1123–1137. [[CrossRef](#)]
4. Gronemeyer, P.; Ditz, R.; Strube, J. Trends in Upstream and Downstream Process Development for Antibody Manufacturing. *Bioengineering* **2014**, *1*, 188–212. [[CrossRef](#)] [[PubMed](#)]
5. Kelley, B. Very large scale monoclonal antibody purification: The case for conventional unit operations. *Biotechnol. Prog.* **2007**, *23*, 995–1008. [[CrossRef](#)] [[PubMed](#)]
6. Strube, J.; Ditz, R.; Kornecki, M.; Huter, M.; Schmidt, A.; Thiess, H.; Zobel-Roos, S. Process intensification in biologics manufacturing. *Chem. Eng. Process. Process Intensif.* **2018**, *133*, 278–293. [[CrossRef](#)]

7. Strube, J.; Grote, F.; Ditz, R. Bioprocess Design and Production Technology for the Future. In *Biopharmaceutical Production Technology*; Wiley-VCH Verlag GmbH & Co. KGaA: Weinheim, Germany, 2012; pp. 657–705, ISBN 9783527653096.
8. Singh, N.; Arunkumar, A.; Chollangi, S.; Tan, Z.G.; Borys, M.; Li, Z.J. Clarification technologies for monoclonal antibody manufacturing processes: Current state and future perspectives. *Biotechnol. Bioeng.* **2016**, *113*, 698–716. [[CrossRef](#)]
9. Jain, E.; Kumar, A. Upstream processes in antibody production: Evaluation of critical parage healthcameters. *Biotechnol. Adv.* **2008**, *26*, 46–72. [[CrossRef](#)]
10. Pollock, J.; Ho, S.V.; Farid, S.S. Fed-batch and perfusion culture processes: Economic, environmental, and operational feasibility under uncertainty. *Biotechnol. Bioeng.* **2013**, *110*, 206–219. [[CrossRef](#)]
11. Birch, J.R.; Racher, A.J. Antibody production. *Adv. Drug Deliv. Rev.* **2006**, *58*, 671–685. [[CrossRef](#)]
12. Al-Rubeai, M. *Animal Cell Culture*; Springer International Publishing: Cham, Switzerland, 2015; ISBN 978-3-319-10319-8.
13. GE Healthcare. *Strategies for Protein Purification Handbook*; GE Healthcare LS: Uppsala, Sweden, 2010.
14. *Continuous Biomanufacturing-Innovative Technologies and Methods*; Subramanian, G. (Ed.) Wiley-VCH Verlag GmbH & Co. KGaA: Weinheim, Germany, 2017; ISBN 9783527699902.
15. *Biopharmaceutical Production Technology*; Subramanian, G., Ed.; Wiley-VCH Verlag GmbH & Co. KGaA: Weinheim, Germany, 2012; ISBN 9783527653096.
16. *Bioseparation and Bioprocessing*, 2nd ed.; Subramanian, G., Ed.; Wiley-VCH: Weinheim, Germany, 2007.
17. Rita Costa, A.; Elisa Rodrigues, M.; Henriques, M.; Azeredo, J.; Oliveira, R. Guidelines to cell engineering for monoclonal antibody production. *Eur. J. Pharm. Biopharm.* **2010**, *74*, 127–138. [[CrossRef](#)]
18. Gstraunthaler, G.; Lindl, T. *Zell-und Gewebekultur. Allgemeine Grundlagen und Spezielle Anwendungen*, 7th ed.; Springer: Berlin/Heidelberg, Germany, 2013; ISBN 9783642331121.
19. Gronemeyer, P.; Ditz, R.; Strube, J. Implementation of aqueous two-phase extraction combined with precipitation in a monoclonal antibody manufacturing process. *Chim. Oggi Chem. Today* **2016**, *34*, 66–70.
20. Gronemeyer, P.; Schmidt, A.; Zobel, S.; Strube, J. Efficient Manufacturing of Biologics. *Chem. Ing. Tech.* **2016**, *88*, 1329. [[CrossRef](#)]
21. Gronemeyer, P.; Thiess, H.; Zobel-Roos, S.; Ditz, R.; Strube, J. Integration of Upstream and Downstream in Continuous Biomanufacturing. In *Continuous Biomanufacturing—Innovative Technologies and Methods*; Subramanian, G., Ed.; Wiley-VCH Verlag GmbH & Co. KGaA: Weinheim, Germany, 2017; pp. 481–510, ISBN 9783527699902.
22. Jungbauer, A. Continuous downstream processing of biopharmaceuticals. *Trends Biotechnol.* **2013**, *31*, 479–492. [[CrossRef](#)] [[PubMed](#)]
23. Karst, D.J.; Steinebach, F.; Soos, M.; Morbidelli, M. Process performance and product quality in an integrated continuous antibody production process. *Biotechnol. Bioeng.* **2016**, *114*, 298–307. [[CrossRef](#)] [[PubMed](#)]
24. Konstantinov, K.B.; Cooney, C.L. White Paper on Continuous Bioprocessing May 20–21 2014 Continuous Manufacturing Symposium. *J. Pharm. Sci.* **2015**, *104*, 813–820. [[CrossRef](#)] [[PubMed](#)]
25. Karst, D.J.; Serra, E.; Villiger, T.K.; Soos, M.; Morbidelli, M. Characterization and comparison of ATF and TFF in stirred bioreactors for continuous mammalian cell culture processes. *Biochem. Eng. J.* **2016**, *110*, 17–26. [[CrossRef](#)]
26. Warikoo, V.; Godawat, R.; Brower, K.; Jain, S.; Cummings, D.; Simons, E.; Johnson, T.; Walther, J.; Yu, M.; Wright, B.; et al. Integrated continuous production of recombinant therapeutic proteins. *Biotechnol. Bioeng.* **2012**, *109*, 3018–3029. [[CrossRef](#)] [[PubMed](#)]
27. Zydney, A.L. Continuous downstream processing for high value biological products: A Review. *Biotechnol. Bioeng.* **2016**, *113*, 465–475. [[CrossRef](#)] [[PubMed](#)]
28. Hernandez, R. Continuous Manufacturing: A Changing Processing Paradigm. *BioPharm Int.* **2015**, *28*, 20–27.
29. Montgomery, A.; Scott, C.; Center, A. *Continuous Chromatography. Experts Weigh in on the Possibilities and the Reality*; BioProcess International: Boston, MA, USA, 2019.
30. Thiess, H.; Zobel-Roos, S.; Gronemeyer, P.; Ditz, R.; Strube, J. Engineering Challenges of Continuous Biomanufacturing Processes (CBP). In *Continuous Biomanufacturing-Innovative Technologies and Methods*; Subramanian, G., Ed.; Wiley-VCH Verlag GmbH & Co. KGaA: Weinheim, Germany, 2017; pp. 69–106, ISBN 9783527699902.

31. Steinebach, F.; Ulmer, N.; Wolf, M.; Decker, L.; Schneider, V.; Walchli, R.; Karst, D.; Souquet, J.; Morbidelli, M. Design and operation of a continuous integrated monoclonal antibody production process. *Biotechnol. Prog.* **2017**, *33*, 1303–1313. [CrossRef]
32. Kateja, N.; Kumar, D.; Sethi, S.; Rathore, A.S. Non-protein a purification platform for continuous processing of monoclonal antibody therapeutics. *J. Chromatogr. A* **2018**, *1579*, 60–72. [CrossRef] [PubMed]
33. Whitford, W.; GE Healthcare. Continuous Biomanufacturing: 10 Reasons Sponsors Hesitate. Available online: <https://www.bioprocessonline.com/doc/continuous-biomanufacturing-reason-sponsors-hesitate-0001> (accessed on 16 May 2019).
34. ICH Expert Working Group. Pharmaceutical Development Q8(R2). In *ICH Harmonised Tripartite Guideline; International Council for Harmonisation of Technical Requirements for Pharmaceuticals for Human Use*: Geneva, Switzerland, 2009; pp. 1–28.
35. ICH Expert Working Group. Specifications: Test Procedures and Acceptance Criteria for Biotechnological/Biological Products Q6b. In *Ich Harmonised Tripartite Guideline; International Council for Harmonisation of Technical Requirements for Pharmaceuticals for Human Use*: Geneva, Switzerland, 1999; pp. 1–20.
36. FDA. Guidance for Industry. PAT—A Framework for Innovative Pharmaceutical Development, Manufacturing, and Quality Assurance. 2004. Available online: <https://www.fda.gov/downloads/drugs/guidances/ucm070305.pdf> (accessed on 19 February 2018).
37. ICH Expert Working Group. *ICH Guideline Q9 on Quality Risk Management; Step 4*; International Council for Harmonisation of Technical Requirements for Pharmaceuticals for Human Use: Geneva, Switzerland, 2005; 408p.
38. Uhlenbrock, L.; Sixt, M.; Strube, J. Quality-by-Design (QbD) process evaluation for phytopharmaceuticals on the example of 10-deacetylbaccatin III from yew. *Resour. Effic. Technol.* **2017**, *3*, 137–143. [CrossRef]
39. Alt, N.; Zhang, T.Y.; Motchnik, P.; Taticek, R.; Quarmby, V.; Schlothauer, T.; Beck, H.; Emrich, T.; Harris, R.J. Determination of critical quality attributes for monoclonal antibodies using quality by design principles. *Biologicals* **2016**, *44*, 291–305. [CrossRef] [PubMed]
40. Croughan, M.S.; Konstantinov, K.B.; Cooney, C. The future of industrial bioprocessing: Batch or continuous? *Biotechnol. Bioeng.* **2015**, *112*, 648–651. [CrossRef] [PubMed]
41. Schmidt, A.; Richter, M.; Rudolph, F.; Strube, J. Integration of Aqueous Two-Phase Extraction as Cell Harvest and Capture Operation in the Manufacturing Process of Monoclonal Antibodies. *Antibodies* **2017**, *6*, 21. [CrossRef]
42. *Ullmann's Encyclopedia of Industrial Chemistry*; Wiley-VCH Verlag GmbH & Co. KGaA: Weinheim, Germany, 2000; ISBN 9783527306732.
43. Strube, J.; Zobel-Roos, S.; Ditz, R. Process-Scale Chromatography. In *Ullmann's Encyclopedia of Industrial Chemistry*; Wiley-VCH Verlag GmbH & Co. KGaA: Weinheim, Germany, 2000; pp. 1–47, ISBN 3527306730.
44. Zobel-Roos, S.; Thiess, H.; Gronemeyer, P.; Ditz, R.; Strube, J. Continuous Chromatography as a Fully Integrated Process in Continuous Biomanufacturing. In *Continuous Biomanufacturing-Innovative Technologies and Methods*; Subramanian, G., Ed.; Wiley-VCH Verlag GmbH & Co. KGaA: Weinheim, Germany, 2017; pp. 369–392, ISBN 9783527699902.
45. Sixt, M.; Uhlenbrock, L.; Strube, J. Toward a Distinct and Quantitative Validation Method for Predictive Process Modelling—On the Example of Solid-Liquid Extraction Processes of Complex Plant Extracts. *Processes* **2018**, *6*, 66. [CrossRef]
46. Kornecki, M.; Strube, J. Accelerating Biologics Manufacturing by Upstream Process Modelling. *Processes* **2019**, *7*, 166. [CrossRef]
47. Schmidt, A.; Strube, J. Distinct and Quantitative Validation Method for Predictive Process Modeling with Examples of Liquid-Liquid Extraction Processes of Complex Feed Mixtures. *Processes* **2019**, *7*, 298. [CrossRef]
48. Huter, M.; Strube, J. Model-based Design and Process Optimization of Continuous Single Pass Tangential Flow Filtration Focusing on Continuous Bioprocessing. *Processes* **2019**, *7*, 317. [CrossRef]
49. Wechselberger, P.; Seifert, A.; Herwig, C. PAT method to gather bioprocess parameters in real-time using simple input variables and first principle relationships. *Chem. Eng. Sci.* **2010**, *65*, 5734–5746. [CrossRef]
50. Junker, B.H.; Wang, H.Y. Bioprocess monitoring and computer control: Key roots of the current PAT initiative. *Biotechnol. Bioeng.* **2006**, *95*, 226–261. [CrossRef] [PubMed]
51. Alford, J.S. Bioprocess control: Advances and challenges. *Comput. Chem. Eng.* **2005**, *30*, 1464–1475. [CrossRef]

52. Kornecki, M.; Strube, J. Process Analytical Technology for Advanced Process Control in Biologics Manufacturing with the Aid of Macroscopic Kinetic Modeling. *Bioengineering* **2018**, *5*, 25. [[CrossRef](#)] [[PubMed](#)]
53. Zobel-Roos, S.; Mouellef, M.; Siemers, C.; Strube, J. Process Analytical Approach towards Quality Controlled Process Automation for the Downstream of Protein Mixtures by Inline Concentration Measurements Based on Ultraviolet/Visible Light (UV/VIS) Spectral Analysis. *Antibodies* **2017**, *6*, 24. [[CrossRef](#)]
54. Kornecki, M.; Mestmäcker, F.; Zobel-Roos, S.; Heikaus de Figueiredo, L.; Schlüter, H.; Strube, J. Host Cell Proteins in Biologics Manufacturing: The Good, the Bad, and the Ugly. *Antibodies* **2017**, *6*, 13. [[CrossRef](#)]
55. Lewis, L.M.; Johnson, R.E.; Oldroyd, M.E.; Ahmed, S.S.; Joseph, L.; Saracovan, I.; Sinha, S. Characterizing the Freeze–Drying Behavior of Model Protein Formulations. *AAPS PharmSciTech* **2010**, *11*, 1580–1590. [[CrossRef](#)]
56. Zobel, S.; Helling, C.; Ditz, R.; Strube, J. Design and operation of continuous countercurrent chromatography in biotechnological production. *Ind. Eng. Chem. Res.* **2014**, *53*, 9169–9185. [[CrossRef](#)]
57. Zobel-Roos, S.; Stein, D.; Strube, J. Evaluation of Continuous Membrane Chromatography Concepts with an Enhanced Process Simulation Approach. *Antibodies* **2018**, *7*, 13. [[CrossRef](#)]
58. Zobel-Roos, S.; Schmidt, A.; Mestmäcker, F.; Mouellef, M.; Huter, M.; Uhlenbrock, L.; Kornecki, M.; Lohmann, L.; Ditz, R.; Strube, J. Accelerating Biologics Manufacturing by Modeling or: Is Approval under the QbD and PAT Approaches Demanded by Authorities Acceptable without a Digital-Twin? *Processes* **2019**, *7*, 94. [[CrossRef](#)]



© 2019 by the authors. Licensee MDPI, Basel, Switzerland. This article is an open access article distributed under the terms and conditions of the Creative Commons Attribution (CC BY) license (<http://creativecommons.org/licenses/by/4.0/>).